HHS Public Access

Author manuscript

Int J Radiat Oncol Biol Phys. Author manuscript; available in PMC 2016 July 06.

Published in final edited form as:

Int J Radiat Oncol Biol Phys. 2015 November 1; 93(3): 588–596. doi:10.1016/j.ijrobp.2015.07.2275.

Combination of gold nanoparticle-conjugated TNF-α and radiation therapy results in a synergistic anti-tumor response in murine carcinoma models

Nathan A. Koonce[1], **Matthew C. Quick**[2], **Matthew E. Hardee**[1], **Azemat Jamshidi-Parsian**[1], **Judith A. Dent**[1], **Giulio F. Paciotti**[3], **Dmitry Nedosekin**[4], **Ruud P.M. Dings**[1], and **Robert J. Griffin**[1]

[1]Department of Radiation Oncology, University of Arkansas for Medical Sciences, Little Rock, AR

[2]Department of Pathology, University of Arkansas for Medical Sciences, Little Rock, AR

[4]Department of Otolarangology, University of Arkansas for Medical Sciences, Little Rock, AR

[3]CytImmune Sciences, Rockville, MD

Abstract

Introduction—Although remarkable preclinical antitumor effects have been shown for tumor necrosis factor-α (TNF) alone and in combination with radiation, clinical use is hindered by systemic dose-limiting toxicities. Here, we investigated the physiological and anti-tumor effects of radiotherapy combined with the novel nanomedicine CYT-6091, a 27-nm average diameter polyethylene glycol-TNF coated gold nanoparticle which passed through Phase I trials recently.

Methods—Physiological and anti-tumor effects of single and fractionated radiation in combination with CYT-6091 were studied in the murine 4T1 breast carcinoma and SCCVII head and neck tumor squamous cell carcinoma models.

Results—In the 4T1 murine breast tumor model we observed a significant reduction in tumor interstitial fluid pressure (IFP) 24h after CYT-6091 alone and combined with a radiation dose of 12 Gy ($p<0.05$ vs control), whereas radiation alone (12Gy) had negligible effect on IFP. In the SCCVII head and neck tumor model, the baseline IFP was not markedly elevated and there was little additional change in IFP post single dose radiation or combined therapy ($p>0.05$ vs control) despite extensive observed vascular damage. The IFP reduction in the 4T1 model was also associated with marked vascular damage and extravasation of red blood cells into the tumor interstitium. A sustained reduction in tumor cell density was observed in the combined therapy group compared to all other groups ($p<0.05$). Finally, we observed a >2-fold delay in tumor growth when CYT-6091 was combined with a single 20 Gy irradiation- notably irrespective of treatment sequence. Moreover, when hypofractionated radiation (12 Gy × 3) was applied in

Correspondence: Robert J. Griffin, 4301 W. Markham Mail Slot #771, Little Rock, AR 72205., RJGriffin@uams.edu.

Conflict of interest: none

combination with CYT-6091 treatment, a >5-fold growth delay was observed in the combined treatment group of both tumor models and determined to be synergistic.

Conclusions—Our results demonstrate that gold-labeled TNF nanoparticles in combination with single or fractionated high-dose radiation therapy is effective in reducing interstitial fluid pressure and tumor growth and shows promise for clinical translation.

Keywords

nanoparticles; radiation therapy; TNF-α; anti-vascular effects; 4T1breast cancer; SCCVII head and neck cancer; nanomedicine

Introduction

Tumor necrosis factor-α (TNF) was initially characterized as the active component in endotoxin-induced hemorrhagic necrosis of transplanted tumors [1]. TNF has since been described as a pleiotropic cytokine with diverse cellular and immunological properties and associated pathologies [2]. Administration of recombinant human TNF (rhTNF) has been investigated for treatment of solid tumors due to vascular damaging and immune stimulating properties of the protein. As an anti-tumor drug, TNF has been limited clinically due to systemic toxicity [3-6], giving rise to the need for a selective tumor delivery mechanism.

In clinical studies, the most successful approach to reduce systemic effects of TNF has been via loco-regional administration using the isolated limb perfusion (ILP) technique [7], which has demonstrated reduced toxicity while maintaining anti-tumor efficacy when combined with chemotherapy. Due to the design of the ILP technique, it is primarily restricted to rare tumors of the extremities. Subsequent strategies have attempted to maintain this robust anti-tumor effect, while circumventing systemic toxicities via advanced targeting, e.g. by antibody or peptide-drug conjugates as well as gene therapy [8-11]. Reports of observed synergy from TNF and radiation therapy have also been reported yet associated toxicities limited these trials from progressing clinically thus far [12-14].

A novel polyethylene glycol (PEG) coated gold nanoparticle formulation was developed to systemically administer TNF, CYT-6091 [15]. A Phase I study confirmed a safe toxicity profile [16] and plans for a Phase II trial are underway. Data has indicated a preferential uptake of CYT-6091 in models of colon, breast and prostate cancer [15, 17, 18]. Similarly, tumor sequestering of CYT-6091 was 2-fold higher compared to AuPEG nanoparticles alone; and, increased TNF accumulation from CYT-6091 was found in tumor tissue compared with normal tissues over time[18].

TNF antineoplastic therapy has primarily shown success in an adjuvant setting, in combination with chemo- or radiation therapy. Preclinical data indicates an improved delivery of chemotherapeutic agents following CYT-6091 therapy [19, 20] however; it is unknown to what extent radiotherapy may benefit from the nanoparticle based-TNF therapy. Due to encouraging results on reduced toxicity while retaining biological efficacy, here we investigated the anti-tumor and tumor physiological effects of CYT-6091 in combination with radiation.

Materials and Methods

Chemical

Water-soluble CYT-6091 was generated in a commercial GLP lab by simultaneously binding rhTNF and thiolated polyethylene glycol to the surface of 27-nm colloidal gold particles. Characterization of CYT-6091 was performed by CytImmune, Inc and has been previously reported[15, 16].

Cell lines and tumor model

Murine mammary carcinoma cells, 4T1, and murine squamous cell carcinoma, SCCVII, cells were cultured at 37 °C and 5% CO_2 in DMEM/F12 50-50 (Mediatech Inc., Manassas, VA) supplemented with 10% BCS. For tumor inoculation, cells at 80% confluence were harvested with 0.125% trypsin/EDTA. 4T1 or SCCVII cells were resuspended in serum free media at 2-4 × 10^5 cells/0.05 mL and implanted subcutaneously in the right rear limb of 2-4 month old female Balb/c mice (Charles River Laboratories) or three-month-old female C3H mice (Jackson Labs), respectively. Cell lines tested negative for mycoplasma.

High-dose single-fraction radiotherapy (4T1)—Rear limb tumors were grown to an average size of 150 mm^3 and randomized to various treatment groups. Treatment groups included: control (n=15), CYT-6091 (250 μg/kg; n=6), radiation (20 Gy; n=8), radiation + CYT-6091 concurrently (n=8), radiation + CYT-6091 24 hrs post-radiation (n=7), and radiation + CYT-6091 30 minutes prior to radiation (n=7).

Fractionated radiotherapy (4T1 and SCCVII)—Rear limb tumors were grown to an average size of 425 mm^3 and randomized to various treatment groups: control (SCCVII, n = 3; 4T1, n = 6), CYT-6091 (250 μg/kg q2d×2; n = 6), radiation (12 Gy q2d×3; SCCVII, n = 5; 4T1, n = 6), and combination (n=5). In the combined treatment group, CYT-6091 was administered immediately after the first two radiation doses. Animals were covered with lead and the tumors extended into the X-ray field using a Faxitron X-ray cabinet system (CP-160, Faxitron X-Ray Corp., W heeling, IL) at a dose rate of 1.079Gy/min (150 kVp and 6.6 mA) under ketamine/xylazine anesthesia. CYT-6091, dissolved in water, was administered i.v. via the tail vein at 250 μg/kg. Tumor measurements were performed with calipers and tumor volumes estimated with the formula $a^2b/2$. See supplemental information for synergy and growth delay details.

Interstitial fluid pressure (IFP) monitoring

Pressure measurements were monitored with a SPR-671 Mikro-Tip catheter transducer (Millar Instruments, Houston, TX) and recorded in ADInstruments Lab Chart software (ADInstruments, Colorado Springs, CO). Pressure readings were recorded for up to 5 min and the average pressure was obtained during a 1-2 minute period of stable pressure readings. IFP was measured 24 h prior to therapy (control) and 24 h after a single treatment of radiation (12 Gy), CYT-6091 or combination.

Histology and pathology analysis

Tumor tissue was harvested at 24 hours and 7 days post treatment, n = 2 - 3 tumors per group, bisected and fixed in 10% neutral buffered formalin. Tissues were paraffin embedded and cut at 5 μm and stained with hematoxylin and eosin (H&E). Images were obtained with a Nikon Eclipse E600 equipped with a Nikon DS-Fi1 camera.

Tumor cell nuclei counting

To quantify changes in tumor cell density observed in response to therapy, nuclear cell counts were performed using Image J (NIH, Bethesda, MD). H&E stains in the 4T1 fractionated radiotherapy study were imaged at 40×, selecting 2 regions per tumor most representative of “normal” tumor tissue for each individual treatment group. Areas of necrosis or hemorrhage were intentionally avoided. Using the cell counter plugin, individual nuclei were manually counted using the original H&E as a guide to exclude obvious neutrophil infiltrate or other potential artifacts.

Statistical analysis

A one-way ANOVA with post-hoc Tukey's multiple comparisons was used to analyze results.

Results

CYT-6091 effectively decreases IFP in breast cancer

In the 4T1 tumor model, the IFP in the tumor of untreated mice was 37 ± 6.6 mmHg. A single dose of 12 Gy radiation caused a modest but not statistically significant drop of 19.5% in IFP compared to control (from 37 to 29.8 mmHg; $p>0.05$) measured at 24 h post exposure. CYT-6091 alone resulted in a significant drop of 82% at 24 h after injection compared to control (from 37 to 6.6 mmHg), whereas the combination caused a 98.6% drop (from 37 to 0.5 mmHg) as compared to the control tumors ($p<0.05$; Figure 1A).

This marked effect on the IFP correlated at the macroscopic and microscopic level with substantial vascular events. Histology from CYT-6091 and combined CYT-6091 and radiation therapy showed red blood cell (RBC) extravasation, indicating vascular damage with resultant hemorrhage by 24 hrs after treatment (Figure 1B). We further investigated IFP in the SCCVII head and neck squamous cell carcinoma. The IFP in SCCVII tumors was found to be over 3-fold lower than 4T1 tumors and there was not a noticeable further decrease in IFP post-treatment with either radiation (8.5 ± 3.4 v. 11.2 ± 4.8 mmHg) or combined therapy (12 ± 2.9 v. 10.3 ± 3.7 mmHg) likely due to the lower IFP in control SCCVII tumors (Figure 1C&D).

CYT-6091 synergistically enhances radiotherapy

Three different combination schedules were tested to investigate the temporal dependence of CYT-6091 to enhance radiation-induced growth delay, relative to radiation alone. Experimental groups were i) CYT-6091 preceding radiation treatment (30 minutes prior), ii) immediately following radiation and iii) 24 hours post-radiation treatment (Figure 2A). CYT-6091 alone had no tumor growth inhibiting effect, whereas radiation alone induced a

1.8-fold delay in tumor growth. Tumors treated with the three different combination schedules produced increased growth delay values ranging from 2.2-2.4-fold (day 5 v. day 11-12) (Figure 2A and Supplemental Table 1).

We further explored an approach relevant to clinical stereotactic body radiation therapy: combination of CYT-6091 treatment with a hypofractionated radiation regimen. Radiation was administered in three fractions of 12 Gy every other day (q2d×3) with CYT-6091 (250μg/kg) injected i.v. immediately following the first two radiation doses (concomitant chemoradiotherapy). Tail vein condition prohibited administration of a third CYT-6091 dose. Similar to the monotherapy, CYT-6091 administered in two doses had little effect on tumor growth (Figure 2B). Compared to control, fractionated radiation alone delayed tumor growth by 2-fold (4 days v. 8 days). In the combination regimen, the tumor growth inhibition of CYT-6091 and radiation was synergistic (Figure 2B and Supplemental Table 2), resulting in an on average tumor growth stasis during the first 14 days. Overall, tumor growth was delayed by 5.3-fold compared to control (4 days v. 21 days).

In the SCCVII head and neck model, radiation was also administered in three fractions of 12 Gy every third day (q3d×3) with CYT-6091 (250μg/kg) injected i.v. immediately following the first two radiation doses. Radiation alone induced a 3.5-fold delay in tumor growth (2 days v 7 days); while the combination therapy induced an 8.5-fold delay in growth (2 days v 17 days; Figure 2C). Plotting the individual growth delay from the combination group revealed that tumor growth was split between 3 tumors that recurred after therapy and 2 tumors that regressed and did not reoccur (Figure 2D).

CYT-6091 selectively damages tumor vasculature and decreases tumor cell density

Direct evidence of vascular disruption and RBC extravasation was observed in tumor tissue from the CYT-6091 alone and the combination treatment group, whereas control and radiation alone did not. This confirmed the gross observations of above mentioned experiments (Figure 1 and Figure 3A). Although the RBCs in the tumor interstitium had resolved in the combination group by day 7, a marked reduction in tumor cell density was observed (Figure 3B and 3C). Tumor cell density was reduced by over 30% in the radiation alone group and by over 50% in the combined CTY-6091 and radiation group compared to untreated control or the CTY-6091 alone group ($p<0.05$).

CYT-6091 disrupts tumor vasculature in hypoxic perinecrotic zones

Histological observations in the 4T1 breast tumor model revealed an evident pattern of vascular disruption in the CYT-6091 treated tumors. RBC extravasation occurred significantly more in the CYT-6091 treated tumors than radiation alone ($p<0.05$) in the region adjacent to necrosis that resulted from central ischemia often observed in this model and tumors of larger sizes (Figure 4A&C). Hypoxia is commonly associated with the perinecrotic tissue zone (pNZ) and staining in control 4T1 tumor tissue for a marker of hypoxia confirmed this aspect (Figure 4B). Hypoxia staining was significantly more intense in the pNZ than in surrounding tissue (Figure D, $p<0.05$).

Discussion

Adjuvant TNF therapy with radiation has shown promise for anti-tumor effects, yet associated dose limiting toxicity (DLT), namely hypotension and hepatotoxicity have tempered the enthusiasm [11, 14]. Our current results show for the first time that gold-nanoparticle conjugated TNF therapy, CYT-6091, is an ideal platform to restore the excitement for clinical application as preclinical and clinical testing reveal that CYT-6091 does not induce the DLTs reported with native TNF treatment.[16] Similar to free TNF alone, CYT-6091 causes tumor selective vascular events that severely impair blood flow within the first 4-8 hours after i.v. injection [21]. Although, this vascular shutdown is not permanent [19, 21], this event might be expected to attenuate radiotherapy response due to hypoxia-related cellular protection [22]. Conversely, we have observed earlier increases in vascular permeability by CYT-6091 as early as 30 min post CYT-6091 administration (data not shown). Thus, we investigated various scheduling regimens, including a pretreatment dose of CYT-6091 (30 min prior to radiation), preceding any hypoxia attenuation [22], to study the contribution of gold presence or enhanced permeability/oxygenation may have on radiation dose enhancement. Additionally, concurrent administration, as well as CYT-6091 administered 24 hours after radiation therapy was also studied. Surprisingly, growth delay in the three different combination strategies was similar, indicating that treatment efficacy is sequence independent. While there are reports that gold may enhance local radiation doses *in vivo*, the amount of gold required in other studies was significantly higher than the dosages used in the present study by 6 orders of magnitude (g/kg vs. μg/ kg) [23]. This makes it unlikely that any increase in reactive oxygen species or increased production of secondary electrons by gold would have played a key role in enhancing radiation using this nanomedicine. However, increased oxidative stress may result from the ischemia-reperfusion effects of CYT-6091 previously observed [21]. Overall, our results indicate a positive influence on radiation-induced growth delay, which may be obtained in a variety of combined treatment scenarios- an important consideration for the realities of the clinical task of scheduling in oncology.

To mimic a more current clinical therapy approach, we administered CYT-6091 immediately following radiation in a hypofractionated dose regimen. High-dose, low fraction number radiation therapy regimens are rapidly increasing in their utility in modern day radiation oncology, as is the combination of administering agents that may maximize the anti-vascular effects of these radiation doses [24-27]. In our study four out of five (80%) breast tumors treated with combined CYT-6091 and radiation therapy reduced in size through day 12 and continued to be controlled through day 16 of evaluation, despite being of a size attributed to intrinsic radiation resistance (large tumor volume, 375 mm^3) compared to the single-fraction radiotherapy experiment (150 mm^3) [28]. Observations of vascular hemorrhaging were seen in both tumor models treated with the combination of CYT-6091 and radiotherapy. Although, vascular hemorrhaging was also noted by CYT-6091 alone, a ‘single’ insult event (Figures 1, 3 & 4). Either the damage from CYT-6091 alone was not extensive enough on its own to effect tumor growth or, vascular regrowth/repair overshadowed any potential anti-tumor effects that may have ensued. However, potential immune involvement can't be ruled out and further understanding of these observed differences are warranted.

Histological evidence of breast tumor tissues in this study demonstrated a heterogeneous response of tumor vessels to the nanoparticle based TNF therapy, in line with other TNF-based approaches [29]. However, little if any has been reported regarding a subpopulation of tumor vessels that are more or less susceptible to TNF-based therapies. In the current study, an evident pattern of tumor vessel damage was observed in vessels residing in peri-necrotic zones (pNZ) of the 4T1 breast tumor model (Figure 4A&C). Immunohistochemical staining in control tumor tissue for a marker of hypoxia indicated intense positive staining localized to the pNZ (Figure 4B&D). This suggests that combined radiation and CYT-6091 may preferentially act on differing regions of the tumor mass, independent of treatment sequencing which would be highly useful for the realities of clinical oncology. Whereas radiation would have its most profound effects in the normoxic tumor regions, CYT-6091 would act most potently to render hypoxic volumes susceptible to radiation-induced control (Figure 4E, *schematic*). Understanding what other factors or mechanisms are associated with this subpopulation of TNF-responding tumor vessels, or moreover what mitigating factors protect select tumor vessels may have further therapeutic and diagnostic potential. Our results in the SCCVII head and neck tumor model, displayed a notably different hemorrhagic pattern than in the breast model more similar to the pattern caused by other VDAs [30]. A more widespread vascular hemorrhaging and associated necrosis was observed with a viable rim of tumor tissue remaining (Supplemental figure 1).

Additionally, in the present study we show that CYT-6091, alone or in combination with radiation, can reduce the tumor interstitial fluid pressure (IFP) in the first 24 h after treatment in the 4T1 model that had a high baseline pressure. Most notably, the combined CYT-6091 and radiation group had a 98.6% reduction in IFP compared to control, with levels reaching that expected of normal tissue. This is in line with results obtained using other TNF-based therapies [31, 32], and supports the notion that CYT-6091 would improve overall chemotherapy access to malignant tissue via enhanced delivery due to this significant reduction in tumor IFP [19, 20]. While IFP is multifactorial in nature [33], Boucher et al. reported microvascular pressure is the principal driving force for increased tumoral IFP. Indeed, the increase in vascular leakage following CYT-6091 therapy, one contributing factor to IFP, led to a significant decrease in IFP and supports the role of microvascular pressure as a key contributor to high IFP. However, we cannot rule out other possibilities including a reduced imbalance of functional blood vessel to functional lymphatic vessel. Regardless, if this lower IFP persists throughout a therapeutic regimen in the clinic, chemotherapy and radiotherapy would be expected to have increased effectiveness all around [34].

Conclusions

Clinical results indicated that systemic administration of TNF is not viable due to dose-limiting toxicities however, the novel nanoparticle formulation of TNF (CYT-6091) used in this study was well tolerated in a Phase I clinical trial. Here, we observed synergistic enhancement of tumor growth inhibition in breast and head and neck cancer models in the first preclinical study to combine CYT-6091 with radiation. CYT-6091 treatment results in reduced tumor interstitial fluid pressure to levels found in normal tissue, suggesting that adjuvant chemotherapy delivery may also be improved with use of this agent. Overall, the current study highlights the potency of CYT-6091 to manipulate vascularity and tumor

microenvironment for therapeutic gain when added in the context of current day radiotherapy dosing and holds great promise for future clinical studies.

Supplementary Material

Refer to Web version on PubMed Central for supplementary material.

Literature Cited

1. Carswell EA, Old LJ, Kassel RL, Green S, Fiore N, Williamson B. An endotoxin-induced serum factor that causes necrosis of tumors. Proc Natl Acad Sci U S A. 1975; 72:3666–3670. [PubMed: 1103152]
2. Bradley JR. TNF-mediated inflammatory disease. J Pathol. 2008; 214:149–160. [PubMed: 18161752]
3. Sherman ML, Spriggs DR, Arthur KA, Imamura K, Frei E 3rd, Kufe DW. Recombinant human tumor necrosis factor administered as a five-day continuous infusion in cancer patients: phase I toxicity and effects on lipid metabolism. J Clin Oncol. 1988; 6:344–350. [PubMed: 3339398]
4. Feinberg B, Kurzrock R, Talpaz M, Blick M, Saks S, Gutterman JU. A phase I trial of intravenously-administered recombinant tumor necrosis factor-alpha in cancer patients. J Clin Oncol. 1988; 6:1328–1334. [PubMed: 3411344]
5. Creagan ET, Kovach JS, Moertel CG, Frytak S, Kvols LK. A phase I clinical trial of recombinant human tumor necrosis factor. Cancer. 1988; 62:2467–2471. [PubMed: 3191449]
6. Furman WL, Strother D, McClain K, Bell B, Leventhal B, Pratt CB. Phase I clinical trial of recombinant human tumor necrosis factor in children with refractory solid tumors: a Pediatric Oncology Group study. J Clin Oncol. 1993; 11:2205–2210. [PubMed: 8229135]
7. Lienard D, Ewalenko P, Delmotte JJ, Renard N, Lejeune FJ. High-dose recombinant tumor necrosis factor alpha in combination with interferon gamma and melphalan in isolation perfusion of the limbs for melanoma and sarcoma. J Clin Oncol. 1992; 10:52–60. [PubMed: 1727926]
8. Sacchi A, Gasparri A, Gallo-Stampino C, Toma S, Curnis F, Corti A. Synergistic Antitumor Activity of Cisplatin, Paclitaxel, and Gemcitabine with Tumor Vasculature-Targeted Tumor Necrosis Factor-α. Clinical Cancer Research. 2006; 12:175–182. [PubMed: 16397040]
9. Jiang C, Niu J, Li M, Teng Y, Wang H, Zhang Y. Tumor vasculature-targeted recombinant mutated human TNF-alpha enhanced the antitumor activity of doxorubicin by increasing tumor vessel permeability in mouse xenograft models. PLoS One. 2014; 9:e87036. [PubMed: 24466321]
10. Bauer S, Oosterwijk-Wakka JC, Adrian N, et al. Targeted therapy of renal cell carcinoma: Synergistic activity of cG250-TNF and IFNg. International Journal of Cancer. 2009; 125:115–123. [PubMed: 19384924]
11. Hallahan DE, Mauceri HJ, Seung LP, et al. Spatial and temporal control of gene therapy using ionizing radiation. Nat Med. 1995; 1:786–791. [PubMed: 7585181]
12. Sersa G, Willingham V, Milas L. Anti-tumor effects of tumor necrosis factor alone or combined with radiotherapy. Int J Cancer. 1988; 42:129–134. [PubMed: 3391701]
13. Hallahan DE, Beckett MA, Kufe D, Weichselbaum RR. The interaction between recombinant human tumor necrosis factor and radiation in 13 human tumor cell lines. International Journal of Radiation Oncology*Biology*Physics. 1990; 19:69–74.
14. Hallahan DE, Vokes EE, Rubin SJ, et al. Phase I dose-escalation study of tumor necrosis factor-alpha and concomitant radiation therapy. Cancer J Sci Am. 1995; 1:204–209. [PubMed: 9166477]
15. Paciotti GF, Myer L, Weinreich D, et al. Colloidal gold: a novel nanoparticle vector for tumor directed drug delivery. Drug Deliv. 2004; 11:169–183. [PubMed: 15204636]
16. Libutti SK, Paciotti GF, Byrnes AA, et al. Phase I and pharmacokinetic studies of CYT-6091, a novel PEGylated colloidal gold-rhTNF nanomedicine. Clin Cancer Res. 2010; 16:6139–6149. [PubMed: 20876255]
17. Visaria R, Bischof JC, Loren M, et al. Nanotherapeutics for enhancing thermal therapy of cancer. Int J Hyperthermia. 2007; 23:501–511. [PubMed: 17952764]

18. Goel R, Shah N, Visaria R, Paciotti GF, Bischof JC. Biodistribution of TNF-alpha-coated gold nanoparticles in an in vivo model system. Nanomedicine (Lond). 2009; 4:401–410. [PubMed: 19505243]
19. Shenoi MM, Iltis I, Choi J, et al. Nanoparticle delivered vascular disrupting agents (VDAs): use of TNF-alpha conjugated gold nanoparticles for multimodal cancer therapy. Mol Pharm. 2013; 10:1683–1694. [PubMed: 23544801]
20. Farma JM, Puhlmann M, Soriano PA, et al. Direct evidence for rapid and selective induction o f tumor neovascular permeability by tumor necrosis factor and a novel derivative, colloidal gold bound tumor necrosis factor. Int J Cancer. 2007; 120:2474–2480. [PubMed: 17330231]
21. Visaria RK, Griffin RJ, Williams BW, et al. Enhancement of tumor thermal therapy using gold nanoparticle-assisted tumor necrosis factor-alpha delivery. Mol Cancer Ther. 2006; 5:1014–1020. [PubMed: 16648573]
22. Chaplin DJ, Durand RE, Olive PL. Acute hypoxia in tumors: implications for modifiers of radiation effects. Int J Radiat Oncol Biol Phys. 1986; 12:1279–1282. [PubMed: 3759546]
23. Hainfeld JF, Slatkin DN, Smilowitz HM. The use of gold nanoparticles to enhance radiotherapy in mice. Phys Med Biol. 2004; 49:N309–315. [PubMed: 15509078]
24. Hallac RR, Zhou H, Pidikiti R, et al. Correlations of noninvasive BOLD and TOLD MRI with pO2 and relevance to tumor radiation response. Magn Reson Med. 2014; 71:1863–1873. [PubMed: 23813468]
25. Song CW, Park I, Cho LC, et al. Is Indirect Cell Death Involved in Response of Tumors to Stereotactic Radiosurgery and Stereotactic Body Radiation Therapy? Int J Radiat Oncol Biol Phys. 2014; 89:924–925. [PubMed: 24969800]
26. Park HJ, Griffin RJ, Hui S, Levitt SH, Song CW. Radiation-induced vascular damage in tumors: implications of vascular damage in ablative hypofractionated radiotherapy (SBRT and SRS). Radiat Res. 2012; 177:311–327. [PubMed: 22229487]
27. Lasnitzki I. A quantitative analysis of the direct and indirect action of X radiation on malignant cells. Br J Radiol. 1947; 20:240–247. [PubMed: 20243691]
28. Wachsberger P, Burd R, Dicker AP. Tumor Response to Ionizing Radiation Combined with Antiangiogenesis or Vascular Targeting Agents: Exploring Mechanisms of Interaction. Clinical Cancer Research. 2003; 9:1957–1971. [PubMed: 12796357]
29. Mauceri HJ, Hanna NN, Wayne JD, Hallahan DE, Hellman S, Weichselbaum RR. Tumor Necrosis Factor α (TNF-α) Gene Therapy Targeted by Ionizing Radiation Selectively Damages Tumor Vasculature. Cancer Research. 1996; 56:4311–4314. [PubMed: 8813113]
30. Horsman MR, Siemann DW. Pathophysiologic effects of vascular-targeting agents and the implications for combination with conventional therapies. Cancer Res. 2006; 66:11520–11539. [PubMed: 17178843]
31. Kristensen CA, Nozue M, Boucher Y, Jain RK. Reduction of interstitial fluid pressure after TNF-alpha treatment of three human melanoma xenografts. Br J Cancer. 1996; 74:533–536. [PubMed: 8761366]
32. Fukumura D, Jain RK. Tumor microenvironment abnormalities: causes, consequences, and strategies to normalize. J Cell Biochem. 2007; 101:937–949. [PubMed: 17171643]
33. Heldin CH, Rubin K, Pietras K, Ostman A. High interstitial fluid pressure an obstacle in cancer therapy. Nat Rev Cancer. 2004; 4:806–813. [PubMed: 15510161]
34. Rofstad EK, Gaustad JV, Brurberg KG, Mathiesen B, Galappathi K, Simonsen TG. Radiocurability is associated with interstitial fluid pressure in human tumor xenografts. Neoplasia. 2009; 11:1243–1251. [PubMed: 19881960]

Summary

Clinical results indicated that systemic administration of TNF is hampered by dose-limiting toxicities. However, a novel delivery platform, CYT-6091 PEGylated gold nanoparticles incorporating TNF, was well tolerated in recent Phase I trials. Here, we observed synergistic tumor growth inhibition when CYT-6091 is combined with radiation therapy. CYT-6091 also reduced tumor interstitial fluid pressure to levels found in normal tissue and affected a subpopulation of tumor vessels.

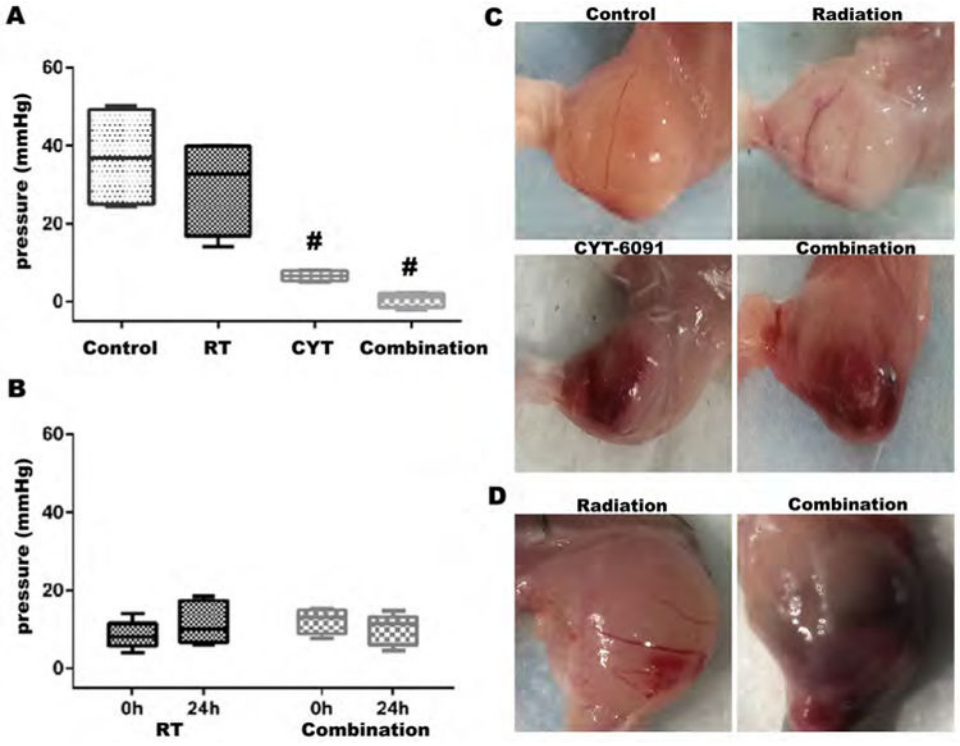

Figure 1. Vascular hemorrhage induction and tumor IFP decreases following CYT-6091 and combined therapy

(A) 4T1 IFP is significantly decreased 24h following therapy in CYT-6091 and combination therapy. Box plots represent min/max and average line (#, $p<0.05$). **(B)** Representative gross images of 4T1 tumor tissue from treatment groups at 24h after treatment. Vascular hemorrhaging was noted in CYT-6091 and combined therapy treatment groups 24 hours following initial therapy. **(C)** SCCVII IFP 24h following combined therapy treatment was relatively unchanged. Box plots represent min/max and mean value. **(D)** Representative gross images of SCCVII tumor tissue from treatment groups at 24h after treatment. Vascular hemorrhaging was noted in the combination therapy group.

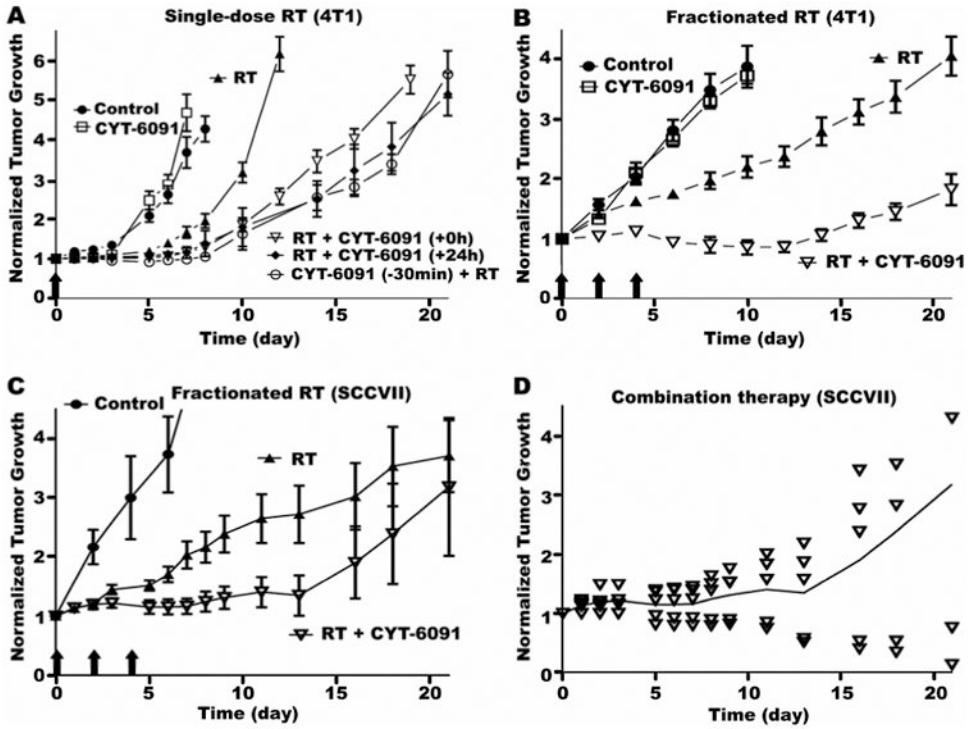

Figure 2. Synergistic tumor growth delay with combined CYT-6091 and radiation independent of scheduling

A) 4T1 tumors were left untreated control or treated with CY-6091, a single radiation dose of 20Gy (RT), RT combined with CYT-6091 immediately following radiation (+0h), RT combined with CYT-6091 24h following radiation (+24h), and CYT-6091 30 min prior to RT (-30min). Data plotted as mean ± SEM. **B)** Fractionated radiation dose regimen and multi-dose CYT-6091 schedule in 4T1 tumors left untreated control or treated with CYT-6091, 12 Gy (q2d×3) (RT), and the combination. Data plotted as mean ± SEM. **C)** Fractionated radiation dose regimen and multi-dose CYT-6091 schedule in SCCVII tumors left untreated (control) or treated with 12 Gy radiation (q3d×3) (RT) and the combination. Data plotted as mean ± SEM. **D)** Tumor growth of individual SCCVII tumors treated with combined radiation and CYT-6091.

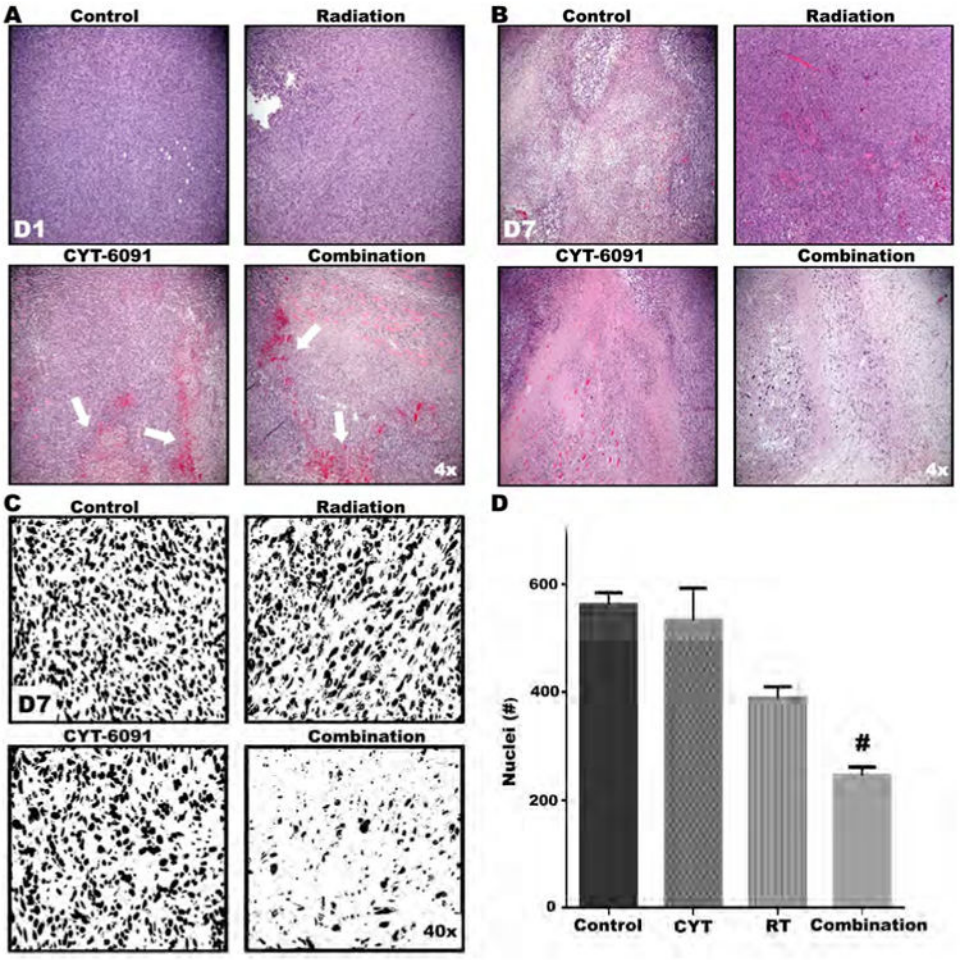

Figure 3. Histological evidence of vascular damage and decreased tumor cell density in 4T1 tumor tissue following combined CYT-6091 and radiation therapy

A) Representative H&E images from treatment groups at time of tissue harvest. At day 1, tumor tissue from CYT-6091 and combined therapy groups displays marked vascular hemorrhaging. **B)** By day 7, tumor cell density in the combined treatment group is markedly reduced. **C)** Representative digitalized and binarized H&E images from treatment groups at day 7. **D)** Symbols above bars indicate significant differences resulting from post-hoc statistical tests. Data represent mean number of nuclei ± SEM (#, $p<0.05$).

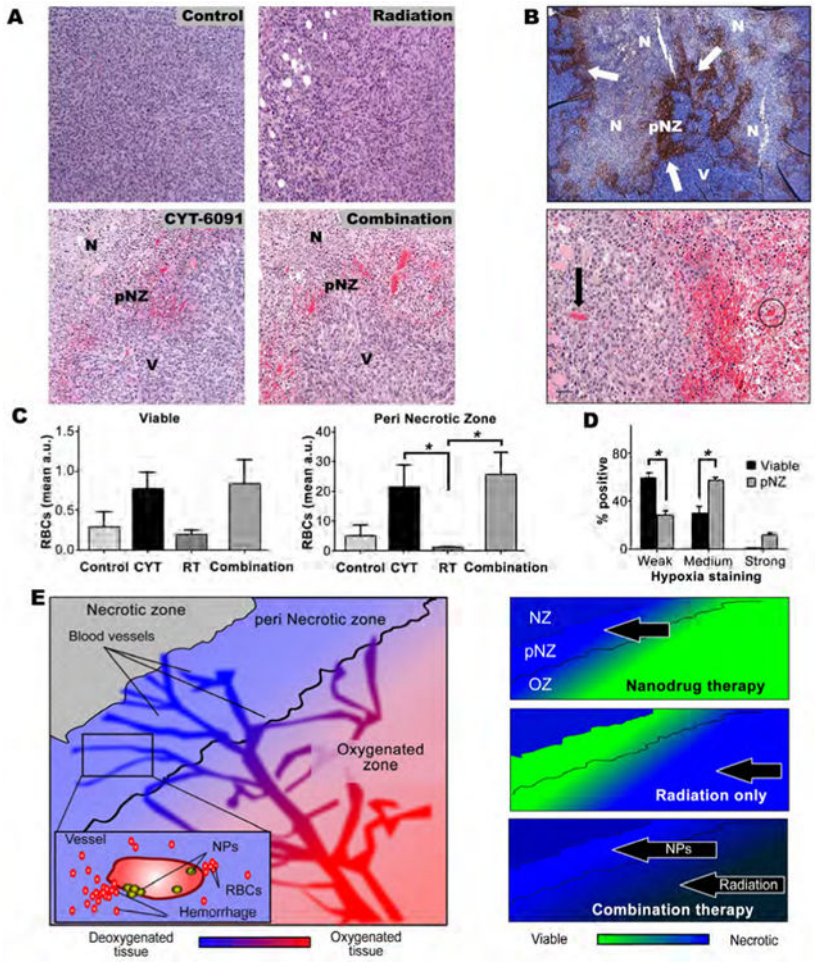

Figure 4. Combined radiation and CYT-6091 therapy effects peri-necrotic tumor vessels in regions of hypoxia

A) Hemorrhaging vasculature is primarily localized to the peri-necrotic zone (pNZ) in both CYT-6091 and combination therapy groups (N = tumor necrosis, V = viable tumor tissue, pNZ = perinecrotic zone). **B)** *(top)* Representative hypoxia staining of untreated 4T1 tumor indicating prominent hypoxia staining in the pNZ. *(bottom)* Dueling vessels - CYT-6091 treated tumors display a differential response to therapy. Arrow points to an unaffected vessel while the circle indicates a vessel damaged by CYT-6091 therapy. **C)** Red blood cell (RBC) extravasation quantified for treatment group in viable tumor tissue (left) and in the pNZ zone (right) (#, $p<0.05$). No significant differences were noted in the viable tumor tissue. **D)** Quantified pimonidazole (hypoxia) staining in pNZ and viable regions of tumor tissue is shown as weak, medium and strong percent positive staining (#, $p<0.05$). **E)** Differential zones of efficacy observed for CYT-6091 + radiation treated 4T1 tumor.